Available online at www.sciencedirect.com
SCIENCE DIRECT®
Computer Networks 50 (2006) 1193–1218
Computer Networks
www.elsevier.com/locate/comnet

Traffic characterization of transport level reliable multicasting: Comparison of epidemic and feedback controlled loss recovery

Öznur Özkasap [a,*], Mine Çağlar [b]

[a] Department of Computer Engineering, Koç University, 34450 Sariyer, Istanbul, Turkey
[b] Department of Mathematics, Koc University, 34450 Sariyer, Istanbul, Turkey

Received 23 June 2004; received in revised form 11 February 2005; accepted 6 June 2005
Available online 8 August 2005

Responsible Editor: G. Morabito

Abstract

Transport level multicast protocols providing reliability and scalability properties are certainly essential building blocks for several distributed group applications. We consider the effect of reliable multicast transport mechanisms on traffic characteristics and hence network performance. Although self-similarity property of unicast traffic, in particular TCP, has been analyzed extensively, multicast traffic has not been incorporated from this perspective. In this study, we focus on traffic characterization of transport level reliable multicasting. In particular, we concentrate on two scalable and reliable multicast protocols as case studies, namely Bimodal Multicast and Scalable Reliable Multicast (SRM), and analyze the traffic generated by them. Our study consists of a complete simulation analysis supported by theoretical work, which shows that self-similarity is protocol dependent. We demonstrate that the Markovian character of Bimodal Multicast's epidemic loss recovery distinguishes an inherently superior protocol. It discretely feeds well-behaved traffic and copes with the existing self-similarity. On the other hand, the feedback controlled loss recovery mechanism of SRM triggers self-similarity. Drawing upon both theoretical and simulation analysis, our results substantiate that transport level can induce long-range dependence even in the absence of application/user level causes.

Keywords: Reliable scalable multicast transport; Traffic characterization; Self-similarity; Long-range dependence; Epidemic communication

* Corresponding author. Tel.: +90 212 338 1584; fax: +90 212 338 1548.
E-mail addresses: oozkasap@ku.edu.tr (Ö. Özkasap), mcaglar@ku.edu.tr (M. Çağlar).

1389-1286/$ - see front matter © 2005 Elsevier B.V. All rights reserved.
doi:10.1016/j.comnet.2005.06.009

1. Introduction

Emerging large-scale distributed group applications such as videoconferencing, multimedia dissemination, instant messaging, and distributed cooperative work have the key requirement of distributing data among participants with application specific quality of service needs. Multicast protocols at the transport and application layers of the network architecture provide efficient communication services for such applications. Although there exist several studies investigating traffic characteristics of unicast communication, multicast traffic has not been examined extensively. Our approach in this article is to focus on scalable and reliable multicast communication through traffic properties.

Two important characteristics of network traffic, *self-similarity* and *long-range dependence* (LRD), are investigated over the last decade as a result of the pioneering work [1]. The existence of these characteristics in a variety of networked environments such as LAN, WAN and ATM as well as isolated traffic sources such as VBR video traffic and WWW traffic have been verified through fine-grained measurements [2]. The mechanisms and dynamics of the network can be related to the observations by theoretical analysis. A review of the theoretical models for unicast communication is given in [3]. The theory predicts that LRD is caused mainly by user and application characteristics; heavy tailed connection times and file sizes, respectively. This has been further confirmed with measurements to close the loop in the analysis. Larger time scales like minutes and hours are affected by application and human causes, whereas at the transport layer, TCP is capable of shaping the traffic at the time scales of few milliseconds to tens of seconds [4,5].

The interest for the identification of self-similarity in data traffic is driven by its adverse consequences on network performance [6]. Although the research in mathematical modeling of traffic has decelerated, network traffic measurements continue for observation of new characteristics. In recent studies, measurements are taken for wireless [7] as well as peer-to-peer traffic [8]. On the other hand, transport level multicast traffic is expected to increase its share in the Internet with increased availability of large-scale group applications. In this paper, we study traffic characterization of transport level reliable multicasting. For this purpose, we focus on two scalable and reliable multicast protocols as case studies, namely Bimodal Multicast and Scalable Reliable Multicast (SRM), and analyze the traffic generated by them through extensive simulations and theoretical work. The former is a reliable transport protocol based on peer-to-peer epidemic principles for loss recovery [9], and the latter is based on feedback suppression through timer parameters similar to TCP [10]. We analyze simulated traces to compare Bimodal Multicast with SRM at both transport and link level measurements. The present paper provides substantial evidence for the prediction in our preliminary studies [11–13] that Bimodal Multicast generates short-range dependent traffic whereas SRM causes long-range dependence. As preliminary work, only short sequences of delay have been analyzed in [11,12].

Our present work consists of a complete analysis and a detailed extension of [13] to reveal the causes behind the protocol performances and different traffic behaviors. The delay sequences are now analyzed in detail for recovered and successful messages. In order to provide an explanation for the simulation results, theoretical delay analysis of Bimodal Multicast is accomplished. More importantly, detailed examination of traffic at the link level is carried out as LRD and self-similarity at the link level have direct consequences on network performance. Other performance measures such as throughput and overhead are also investigated. The effects of system-wide noise rate, background traffic, network topology and self-similar sources are explored. These all demonstrate that the Markovian character of Bimodal Multicast loss recovery distinguishes an inherently superior protocol for multicast communication. Bimodal Multicast feeds well-behaved traffic when isolated, and copes with the existing self-similarity through neither getting affected by nor altering any background traffic. On the other hand, we argue that the loss recovery mechanism of SRM triggers self-similarity. As a more general issue, our results substantiate that transport level can induce LRD even in the absence of application/user level causes.

The article is organized as follows. Section 2 gives terminology and summarizes related work on traffic characterization in relation to transport level reliable multicasting. In Section 3, multicast transport protocols under investigation are reviewed. We give our contributions in Sections 4–8. In Section 4, theoretical analysis of Bimodal Multicast delay and the simulation results for delay are described. Section 5 focuses on multicast traffic at the link level and studies traffic counts from simulations together with an analysis of interarrival distributions. Several performance measures and effect of network topology on the traffic characteristics are explored in Section 6. In Section 7, protocol traffic behavior is investigated in the presence of self-similar background traffic in the network. The case of self-similar sources and strict self-similarity is discussed in Section 8. Finally, Section 9 states our overall conclusions.

2. Terminology and related work

Self-similarity and long-range dependence (LRD) are two important traffic characteristics that we exploit for comparing the performance of the multicast transport protocols in this paper. For the aim of reliable performance analysis, traffic measurements are considered over time intervals where such measurements are statistically stationary. A stochastic process $X = \{X(t) : t \geqslant 0\}$ is called stationary if its probability distribution, and hence all statistical properties, are invariant under its translations in time given by $\{X(t + s) : t \geqslant 0\}$, for each $s \in R$. For example, $X(t)$ can denote the traffic volume at time instant t passing through a link, measured in bits per second, and its distribution will be the same as the distribution of $X(t + s)$, for every s, if the process X is stationary.

Self-similarity can shortly be described as the scale invariance of the bursty behavior, observed ubiquitously in the network traffic. A stationary random process $X = \{X(t) : t \geqslant 0\}$ with autocorrelation function r is said to be *second-order self-similar* with *Hurst* parameter H, $H > 0$, if the process $\{a^{-H}X(at) : t \geqslant 0\}$ has the same correlation structure r as X, for all $a > 0$. In the presence of self-similarity, an appropriate scaling in space compensates for a scaling in time. This can be illustrated as in Fig. 1 which shows one set of link counts obtained from the simulations of the present paper, given later in full length in Fig. 9(d). In this figure, the same data set is displayed over three different time scales while both x- and y-axis of the graphs are rescaled for visual purposes. Burstiness is apparent in all time scales and typically occurs from milliseconds to tens of seconds in the network traffic. In contrast, aggregation of throughput in larger time units would average out the bursts observed in the finest time unit if throughput was a Markov process [1]. This is not the case for self-similar traffic.

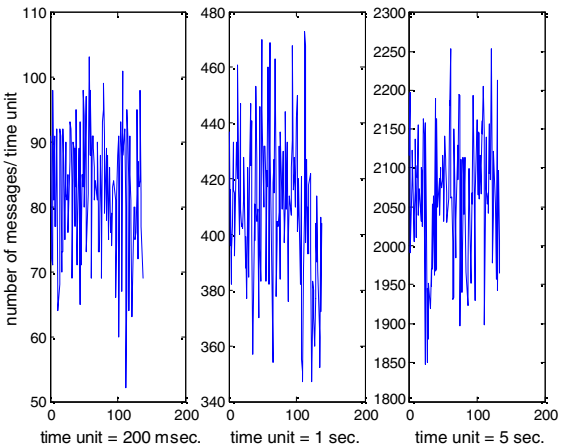

Fig. 1. Illustration of self-similarity: burstiness preserved over a wide range of time scales.

Second order self-similarity is more commonly used in characterizing self-similarity, in contrast to strict self-similarity which is defined in terms of a nonstationary process. In the network traffic context, typically the cumulative traffic volume from time 0 up to time t, say $Y(t)$, is an example of a nonstationary process [14]. Its increments in time, or the derivative process, denoted by $X(t)$ above is typically assumed to be stationary. Formally, a random process $Y = \{Y(t) : t \geqslant 0\}$ is said to be *strictly self-similar* with *Hurst* parameter H, $H > 0$, if the process $\{a^{-H}Y(at) : t \geqslant 0\}$ has the same probability distribution as Y, for all $a > 0$. Strict self-similarity is a very strong

statistical invariance property that holds for all finite dimensional distributions and moments of Y, not just the second-order properties. Besides, Y does not need to have a finite second (or higher) moment for this definition to hold. If it does though, second-order self-similarity definition is applicable for such a nonstationary process as well. If Y is a Gaussian process, then the two definitions are clearly equivalent. Throughout the paper, we work with stationary measurements and use self-similarity in the weaker, second-order sense if not indicated otherwise.

On the other hand, long-range dependence, the close relative of self-similarity, is defined as the slow, hyperbolic decay of the correlation function r of a stationary process X with a finite second moment. The process X is said to be *long-range dependent* if $r(k) \propto k^{-\rho}$ as $k \to \infty$, $0 < \rho < 1$, in contrast to the autocorrelation function of a short-range dependent process which has the form $r(k) \propto \rho^k$, as $k \to \infty$, $0 < \rho < 1$. See Fig. 2 for an illustration of the two different forms of r. It can be seen that the correlation remains significant even for very large time lags, in the presence of LRD. Long-range dependence is characterized through the Hurst parameter H which takes values in $(0.5, 1)$. Analysis reveals that long-range dependence exists ubiquitously in the network traffic in addition to self-similarity with $\rho = 2 - 2H$. However, if the second moments are infinite, only strict self-similarity should be investigated as self-similarity and LRD have separate adverse consequences on the network performance.

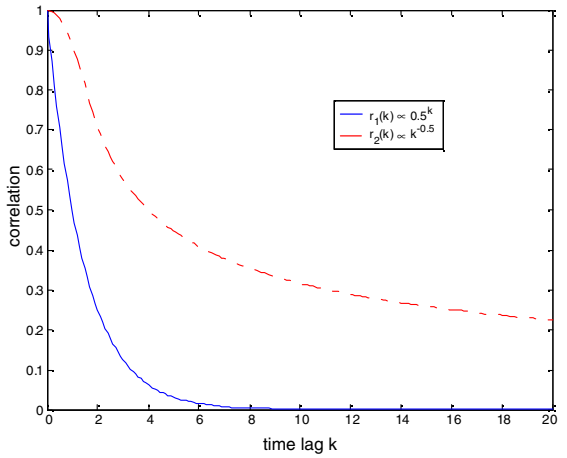

Fig. 2. Examples of correlation functions of a long-range dependent and a short-range dependent process.

In order to estimate the Hurst parameter H of LRD from measured traces, we apply the wavelet estimation method as given in [15] when finite variance (second moment) is indicated for the measurements. In the case of infinite variance, we follow the method of estimation given in [16] for the estimation of H of a strictly self-similar process. LRD is inapplicable in the latter case due to infinite variance. Daubechies wavelets are used in both methods.

The impact and therefore the relevance of self-similarity and LRD depend on the performance metric of interest. For example, it was shown in [17] that a Markov model can be appropriate when short-range dependence is strong, and hence only second-order statistics is sufficient for steady state queuing analysis. However, in certain infinite buffer fluid queues fed by long range dependent on/off sources, the stationary queuing distribution has infinite mean [14]. Such infinite moments disappear if the buffer is finite, intuitively because a finite reservoir cannot hold long memory, but the LRD of the traffic stream strongly affects the buffer overflow loss process. Markov chain models may give good estimates of loss rates and mean buffer sizes under the condition that there is strong short-range dependence in addition to LRD with a not very large Hurst parameter [18]. Similarly, in [19] a Markov model is considered for constant bit rate connections and rate adaptive services such as file transfers, when they share the same link in the network. Although applications such as file transfers can cause self-similarity and LRD [1], the assumptions of exponential connection holding time, or the time scale separation, namely fast set-up and tear down of the connections, of [19] would not yield LRD at the link level traffic. Different models based on a heavy tailed distribution for holding times are more appropriate when long-range dependence is observed in traffic measurements [3]. In particular, Markov modulated Poisson processes can be used to capture the behavior of self-similar traffic in the relevant time scales [20,21].

Long-range dependence has been originally characterized through traffic counts at the link level [1]. Several mathematical models explain the emergence of LRD at the link level as a consequence of the user/application behavior. On the other hand, it has been empirically shown that measurements such as interarrivals between packets, on and off periods, and delay of packets also show LRD when analyzed for Hurst parameter. Certainly, neither the mathematical models of translation of self-similarity from application to link layer nor the empirical results obtained from TCP dominated networks provide the complete picture. There exist recent efforts to incorporate the transport layer to mathematical models of traffic [5,22].

Transport level multicast protocol support for distributed applications is essential due to the fact that large-scale deployment of network level multicast on the Internet has still not been realized. As most of the efforts in multicast studies are focused on developing new protocols and applications, comparative study of multicast protocols can shed light on the effect of transport mechanisms on traffic characteristics and hence network performance. Although self-similarity property of TCP traffic has been analyzed for unicast communication, multicast traffic has not been incorporated from this perspective. These are the main motivation of our work. Our preliminary studies [11–13] rely on the comparison of delay generated by two multicast transport protocols. We see that SRM delay is long-range dependent whereas that of Bimodal Multicast is short-range dependent under identical settings. This is the basis of our further comparative study of traffic at the link level in the present paper for several parameters of the network. We select SRM for comparison to Bimodal Multicast first because SRM with a receiver-initiated approach to loss recovery is fundamentally different from the latter, which has peer-to-peer epidemic approach; second SRM is very similar to TCP, which is prevalent in the present networks. In this paper, we provide empirical evidence to our claim that self-similarity is protocol dependent and support it with theoretical analysis. The questions we ultimately aim to answer are as follows:

- Which multicast protocol(s) can best cope with the existing self-similar traffic and its adverse performance consequences in the WAN/Internet?
- What are the principles and mechanisms behind these protocols that qualify them to be superior/better and discretely feed well-behaved traffic into the existing networks?
- Can these principles be also used for the improvement and/or design of protocols for unicast communication as well as wireless data communication?

3. Multicast transport protocol descriptions

In this section, multicast protocols under investigation are reviewed.

3.1. Bimodal multicast

Bimodal Multicast [9] is a novel option in the spectrum of multicast protocols. It is inspired by prior work on epidemic protocols [23], Muse protocol for network news distribution [24], and the lazy transactional replication method of [25]. The important aspects of Bimodal Multicast are peer-to-peer epidemic loss recovery mechanism, throughput stability guarantee which provides predictable and small variance in the data delivery rate, and a bimodal delivery guarantee. The protocol scales well as the number of participants increases, and in contrast to the other scalable reliable multicast protocols it gives predictable reliability even under highly perturbed conditions. The behavior of Bimodal Multicast can be predicted given simple information on how processes and the network behave most of the time. The protocol exhibits stable throughput under failure scenarios that are common on real large-scale networks [9]. In contrast, this kind of behavior can cause other reliable multicast protocols to exhibit unstable throughput.

Bimodal Multicast consists of two sub-protocols, namely an optimistic dissemination protocol and a two-phase anti-entropy protocol. The former is a best-effort, hierarchical multicast used to efficiently deliver a multicast message to its

destinations. This phase is unreliable and does not attempt to recover a possible message loss. If IP multicast is available in the underlying system, it can be used for this purpose. For instance, the protocol model implemented on ns-2 network simulator [26] in this study is based on IP multicast. Otherwise, a randomized dissemination protocol can play this role. Fig. 3 illustrates the execution of Bimodal Multicast on a simple scenario where there is a six-member multicast group, and node S is the source. As demonstrated in Fig. 3(a), as a result of the first phase that does not provide reliability, some group members may not get a multicast message disseminated by the source due to transient link and/or node failures in the system. In the figure, nodes Q and T fail to receive the initial multicast as indicated by dashed arrows.

The second phase of Bimodal Multicast is responsible for providing reliability via message loss recovery. It is based on an epidemic anti-entropy protocol that detects and corrects inconsistencies in a system by continuous gossiping. The two-phase anti-entropy protocol progresses through unsynchronized rounds in a peer-to-peer manner. According to the terminology of epidemiology, a peer holding information or an update it is willing to share is called *infective*. A peer is called *susceptible* if it has not yet received an update. In the anti-entropy process, non-faulty peers are always either susceptible or infective. One of the fundamental results of epidemic theory shows that simple epidemics eventually infect the entire population. If there is a single infective peer at the beginning, updates will eventually be spread across all peers using anti-entropy. Full infection is achieved in expected time proportional to the logarithm of the group size. Therefore, as a result of the first phase of the protocol, Q and T are susceptible peers, and the other group members are infective since they received the initial multicast. In each round, every peer (group member) randomly selects another group member and sends a digest of its message history via gossiping. Fig. 3(b) illustrates a sample loss recovery round initiated by peer P, where P randomly selects the peer Q, and

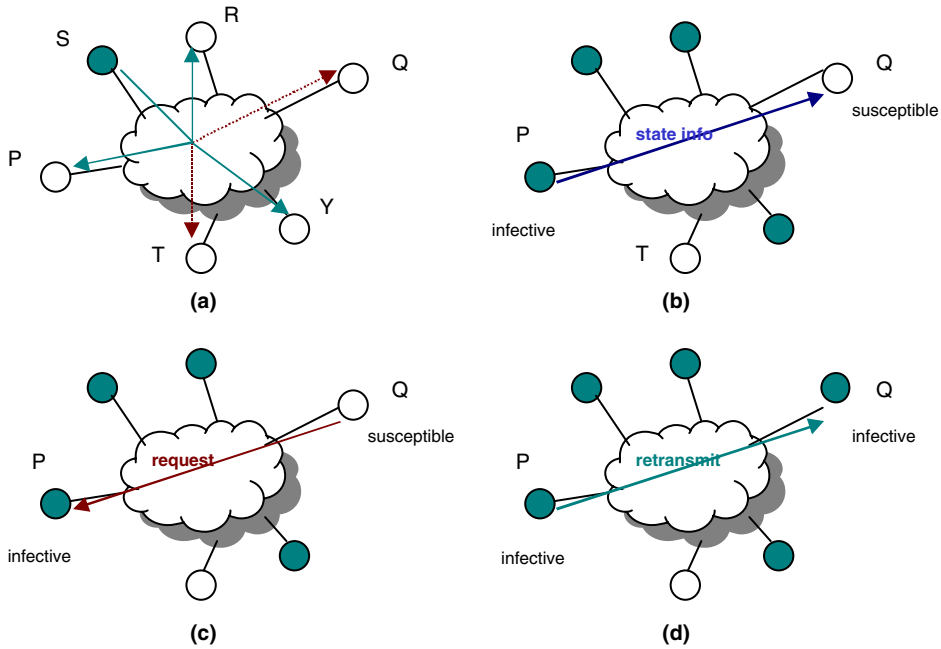

Fig. 3. Bimodal Multicast execution. (a) Optimistic dissemination; (b) loss recovery round initiated by peer P; (c) requesting a message and (d) retransmitting the message.

sends a digest of its current message buffer contents. The digest includes the identifiers of messages in the buffer. The figure simplifies the execution by showing only the round initiated by P. In practice, every group member initiates its own round periodically. The receiving group member Q compares the digest with its own message history. Then, if it is lacking a message, it requests the message from the gossiping member via a request message (Fig. 3(c)). Upon receiving the request, the gossiping member retransmits the requested message to the request owner (Fig. 3(d)) that makes peer Q infective during this sample round. For further details on Bimodal Multicast, we refer interested reader to [9].

3.2. Feedback controlled scalable reliable multicast protocols

Various scalable reliable multicast solutions provide best-effort reliability in large-scale. Example systems are Internet Muse protocol for network news distribution [24], SRM protocol [10], the Pragmatic General Multicast (PGM) protocol [27], and the Reliable Multicast Transport Protocol (RMTP) [28]. These protocols overcome message loss and failures, but they do not guarantee end-to-end reliability. However, Bimodal Multicast provides a form of reliability that can be formally quantified by setting its parameters. It maintains approximate knowledge of the group membership, and does not involve the application in recovery process.

Representative approaches of many existing solutions for providing loss recovery in scalable multicasting are *nonhierarchical feedback control* and *hierarchical feedback control*. The main aim is to reduce the number of feedback messages that are returned to the sender. In the former approach, a model that has been adopted by several wide-area applications is referred to as *feedback suppression*. In the latter approach, hierarchical methods are adopted for achieving scalability for very large groups of receivers [29]. Another alternative for ensuring reliability is *forward error correction* (FEC). The idea behind this approach is predicting losses and transmitting redundant data.

Next, we elaborate on well-known protocols that are based on feedback controlled approaches, and provide comparisons with the epidemic loss recovery. Our study focuses on comparative traffic properties and quantitative analysis of epidemic loss recovery as adopted by Bimodal Multicast and feedback controlled loss recovery as adopted by SRM. In this section, we present qualitative comparison of Bimodal Multicast with hierarchical feedback control approaches of PGM and RMTP as well.

3.2.1. Scalable reliable multicast (SRM)

SRM [10] is a well-known reliable multicast protocol based on feedback suppression. When a receiver detects a message loss, it multicasts its feedback to the rest of the group that in turn allows another group member to suppress its own feedback. A receiver lacking a message schedules a feedback with some random delay. Major novelty of SRM is its use of stochastic mechanisms for feedback suppression. The protocol is rooted in the principles of IP multicast group delivery, application level framing (ALF), adaptivity and robustness in TCP design. SRM dynamically adjusts its control parameters based on the observed performance within a multicast session, which is similar to TCP's adaptive mechanisms for setting timers or congestion control windows. It exploits a receiver-based reliability mechanism, and does not provide ordered delivery of messages. The protocol is designed according to the ALF principle that defers most of the transport level functionality to the application for the purpose of providing flexibility and efficiency in the use of the network.

In SRM, each group member multicasts low rate, periodic session messages that report the sequence number state for active sources, or the highest sequence number received from every member. In addition to state exchange, session messages contain timestamps that are used to estimate the distance from each member to every other to be used by the loss recovery mechanisms. Members also use session messages to determine the current participants of the session. Repair requests and retransmissions are always multicast to the whole group. A lost message ideally triggers only a single request from a host just downstream

of the point of failure. However, SRM can easily encounter situations in which multiple repair messages are multicast in response to a single request. In fact, there is a trade-off in SRM between duplicate message flow and loss recovery speed.

Group members detect message losses by means of gaps in the sequence numbers. When a group member A detects a message loss, it schedules a retransmission request, and sets a request timer to a value from the uniform distribution on

$$[C_1 x d_{S,A}, (C_1 + C_2) x d_{S,A}] \text{ seconds},$$

where $d_{S,A}$ is member A's estimate of the one-way delay to the original source S of the missing data and C_1, C_2 are request timer parameters. If a member receives a request for the missing data before its own request timer for that data expires, then the member resets its request timer. In other words, it suppresses its own request feedback.

When a group member B receives a request from A for a data message that B has a copy, B sets a repair timer to a value from the uniform distribution on

$$[D_1 x d_{A,B}, (D_1 + D_2) x d_{A,B}] \text{ seconds},$$

where $d_{A,B}$ is the B's estimate of the one-way delay to A, and D_1, D_2 are repair timer parameters. If B receives a repair for the missing data before its repair timer expires, then B cancels its repair timer for repair feedback suppression.

3.2.2. Reliable multicast transport protocol (RMTP) and pragmatic general multicast (PGM)

RMTP [28] is based on a hierarchical feedback control approach in which receivers are grouped into local regions. In each local region, there is a special receiver called a Designated Receiver (DR) which is responsible for processing ACKs from receivers in its region, sending ACKs to the sender and retransmitting lost packets. The sender only keeps information on DRs and each DR keeps membership information of its region. This approach reduces the amount of state information kept at the sender, end-to-end retransmission latency due to local receivers taking part in a recovery process and the number of ACKs gathered by the sender. Since only the DRs send their ACKs to the sender, a single ACK is generated per local region and this method for feedback suppression prevents the ACK implosion problem. In addition, hierarchical approach of RMTP eliminates the possible problems of request or repair implosions that can be observed in an SRM session. RMTP uses local recovery by which the effect of a lossy sub-network can be restricted to a small region without affecting the other members of a multicast session. On the other hand, the extra cost of RMTP for providing scalability is additional state kept at the sender and at each DR. A limitation of the protocol especially for dynamic group applications is the static selection of DRs based on approximate location of members.

PGM [27] is a more recent reliable multicast protocol based on a hybrid approach to achieve scalability. The protocol utilizes FEC together with a hierarchical approach as in RMTP and NAK suppression as in SRM. It offers ordered, duplicate-free multicast data delivery, and guarantees that a receiver delivers all data packets or is able to detect unrecoverable data packet loss. PGM is suitable for single source, multiple receiver applications. It employs a NAK-based loss recovery mechanism and similar to Bimodal Multicast it runs over a best effort datagram protocol such as IP multicast. But, PGM also requires router support for constructing hierarchy which would be a limitation for large-scale deployment of the protocol on the Internet. On the other hand, Bimodal Multicast does not require any router support and specific network element, and as a future optimization, the protocol could benefit from a hierarchical structure during epidemic loss recovery.

Overall, SRM, RMTP, PGM and similar feedback controlled approaches are suitable for large-scale networks and they do scale beyond the limits of virtual synchrony protocols offering strong reliability guarantees. When the message loss probability is very low or uncommon, they can give a very high degree of reliability. But, failure scenarios such as router overload and system-wide noise which are known to be common in Internet protocols can cause these protocols to behave pathologically [30,31]. This type of behavior is especially triggered by low-level system-wide noise or transient and high message loss rates. Therefore, reliability properties that these

protocols offer cannot be guaranteed in such failure scenarios. On the other hand, Birman et al. establish that Bimodal Multicast scales well and provides predictable reliability with a steady throughput, even under highly perturbed network conditions [9].

4. Delay analysis

Simulation results reported in [12,13] indicate empirically that both Bimodal Multicast and SRM generate short-range dependent delays for small group sizes, but SRM delays are long-range dependent when the group size is large. In this section, we substantiate our earlier prediction in [13] that the protocol mechanisms are behind this observation through both theoretical and simulation analysis. We theoretically show that Bimodal Multicast's Markovian character is linked to an exponential delay distribution which indicates good network performance. We analyze simulated traces for successful and recovered messages separately to establish that the recovery mechanism of SRM not only causes the LRD of the delays, but also affects the successful message delay distribution. Hence, our simulation results imply degraded network performance for SRM and confirm our theoretical results for Bimodal Multicast.

The delay of a packet or message is calculated as the difference of the deployment time at the sender from the receive time at the receiver. Packet delay measurements over the Internet are used to trace the conditions of the network between an origin and destination pair [32–34]. Delay analysis is important for performance evaluation of the network. There is a direct usage of end-to-end delay as well. For instance, the retransmission timeout parameter of TCP is determined dynamically by packet round-trip delay in the Internet. In our simulations, such measurements represent traffic at the transport level. The randomness in delays is due to noise and the traffic generated by the control and recovery mechanisms of the transport protocol. The measurements are taken after the protocol actions reach a steady state. Hence, the delay measurements form a stationary sequence in simulations below.

4.1. Theoretical analysis of bimodal multicast delay

We aim to characterize the delay distribution of a typical message at a fixed receiver of Bimodal Multicast in this subsection. We show that the marginal delay distribution decays exponentially as expected from Markov property of the epidemic mechanism of Bimodal Multicast. Such a behavior can be modeled through an appropriate chain-binomial framework [35]. Previous analysis in [9] relies on this fact. However, it oversimplifies the delay computations, which are only approximate. Here, we rigorously derive upper bounds for the tail probabilities of the delay distribution.

The gossip stage for a given message of Bimodal Multicast implemented in our simulations goes for 10 rounds before garbage collection, equivalently 1 s. In the analysis below, we assume that the gossip goes forever rather than a fixed number of rounds for a simplification. If gossip stops before the message is delivered to all receivers, there is a possibility that a receiver may not get this particular message. That is why, the delay distribution analyzed here can be considered as that of the received messages.

Consider a fixed message multicast to all group members with an optimistic dissemination protocol from a fixed sender. If it is not received by a group member, it will be repaired through the epidemic mechanism of the protocol. Let N denote the group size and R_t denote the number of receivers that have not received the message at round t. In the epidemic terminology, these are susceptible processes, and equivalently $N - R_t$ corresponds to the number of infectious processes.

At each round, the probability of infection depends on the number of infectious processes present at that time. Let p denote the probability that a particular susceptible process j receives a gossip and the following retransmitted message from a given infectious process i successfully. Then, $q = 1 - p$ is the probability of failure of an infection by that infectious process. Let ε be an upper bound for the probability of message loss for each pair of processes in the network. That is, $0 \leqslant \varepsilon_{ij} \leqslant \varepsilon$ where ε_{ij} is the probability that a message from i to j experiences a send omission failure. Let f denote the fanout defined as the number of

processes a process gossips to at each round. Then, the probability that the infectious process i gossips to the susceptible process j is $\beta = f/N$. For a successful retransmission of the data message, the gossip from i to j, the request message from j to i and the retransmission message from i to j, all associated with the recovery process, must be transmitted successfully. We assume that message loss occurs independently at each stage. It follows that

$$p = \beta(1-\varepsilon_{ij})^2(1-\varepsilon_{ji}) \geqslant \beta(1-\varepsilon)^3$$

and equivalently

$$q \leqslant 1-\beta(1-\varepsilon)^3.$$

We will use $1-\beta(1-\varepsilon)^3$ as a pessimistic value for q. Since each process sends a gossip message to a randomly chosen group member, it is also reasonable to assume that processes get infected independently. Then, the probability that none of the infectious processes at round t infects a susceptible process is q^{N-R_t}. Therefore, the number of susceptible processes in the next round R_{t+1} is Binomially distributed with parameters R_t and q^{N-R_t}. Letting r_{t+1} and r_t be the realizations of R_{t+1} and R_t, respectively, we have

$$P(R_{t+1}=r_{t+1} \mid R_t=r_t) = \binom{r_t}{r_{t+1}} (q^{N-r_t})^{r_{t+1}} (1-q^{N-r_t})^{r_t-r_{t+1}} \quad r_{t+1}=0,1,\ldots,r_t \tag{1}$$

and this probability is 0 if $r_{t+1} > r_t$. As the worst case, it is possible that none of the other group members receive the initial multicast and we have $R_0 = N-1$. In general, it is conditionally a Markov chain on $\{0, 1,\ldots,R_0\}$ given R_0.

Now, let D denote the delay of a message to a fixed receiver, say i. At any round t, we can decide whether the event $\{D \leqslant t\}$ occurred or not by examining the partitions of susceptible and infectious processes. If receiver i is among the infectious processes, then the event has occurred. Due to the homogeneity of the mechanism, its probability is the same for all processes given the current status; it only depends on the number of processes in each partition. That is,

$$P\{D \leqslant t \mid R_t\} = \frac{N-R_t}{N} \quad t=0,1,2,\ldots \tag{2}$$

By taking expectations of both sides, the complementary probability is found as

$$P\{D > t\} = \frac{\mathrm{E}R_t}{N} \quad t=0,1,2,\ldots$$

Here, $P\{D=0\}$ corresponds to the probability that the initial multicast is successful and $P\{D=t\}$, $t=1,2,\ldots$, is the distribution of the delay of the retransmitted messages up to a normalization constant. The delay distribution is hence a mixture of the two distributions as observed in our simulations. Of course, the delay of the successfully transmitted initial multicast has a continuous distribution within the first round depending on the deterministic network parameters. The traffic generated by the retransmitted messages could interfere with this distribution. However, we assume they do not for simplicity and as the simulation results of the previous section indicate noninterference and a mixture type distribution for delay.

We are interested in the distribution of the delay D' of a retransmitted message. That is, the message to receiver i was lost in the initial multicast and is to be repaired through the epidemic mechanism. This is the renormalized distribution given by

$$\begin{aligned} P\{D'=t\} = P\{D=t \mid D>0\} &= \frac{P\{D=t\}}{P\{D>0\}} \\ &= \frac{1}{1-P\{D=0\}} \frac{\mathrm{E}R_{t-1}-\mathrm{E}R_t}{N} \\ &= \frac{1}{\mathrm{E}R_0/N} \frac{\mathrm{E}R_{t-1}-\mathrm{E}R_t}{N} \\ &= \frac{\mathrm{E}R_{t-1}-\mathrm{E}R_t}{ER_0} \quad t=1,2,\ldots \end{aligned}$$

from Eq. (2). Equivalently, the complementary cumulative distribution function is found as

$$\bar{F}(t) \equiv P\{D'>t\} = \frac{\mathrm{E}R_t}{\mathrm{E}R_0} \quad t=1,2,\ldots$$

Now, since R_{t+1} is Binomial with parameters R_t and q^{N-R_t} when given R_t, we have $\mathrm{E}[R_{t+1} \mid R_t] = R_t q^{N-R_t}$, and hence $\mathrm{E}R_{t+1} = \mathrm{E}[R_t q^{N-R_t}]$. But, $q<1$ and R_t is decreasing in t. It follows that $q^{N-R_t} \leqslant q$ almost surely and $\mathrm{E}R_t \leqslant q\mathrm{E}[R_{t-1}]$, $t=1,2,\ldots$ That is, $\mathrm{E}R_t \leqslant q^t \mathrm{E}[R_0]$ and hence

$$\bar{F}(t) \leqslant q^t \quad t=1,2,\ldots$$

which proves that $\bar{F}(t)$ decays faster than a geometric distribution with parameter $p = 1 - q$.

It is possible to derive a stricter upper bound for the tail probability of the delay D'. Note that the transition probability matrix P of R with entries given in (1) is lower triangular and has 1 in the first position in the diagonal, as $P_{00} = P\{R_{t+1} = 0 \mid R_t = 0\} = 1$. Clearly, the eigenvalues of P reside on its diagonal. Since all entries are probabilities, the largest eigenvalue λ_0 is 1. It can be shown that the tail probability of the absorption time τ of the Markov chain R to the absorbing state 0 can be approximated using the second largest eigenvalue λ_1 as

$$P\{\tau > t\} \approx (\text{constant})\lambda_1^t \text{ for large } t.$$

The derivation is similar to that in [36, p. 158]. We sketch the proof. With the pessimistic assumption $R_0 = N - 1$, we have

$$P_i(\tau > t) = \sum_{j=1}^{N-1} P_{ij}^{(t)} = \sum_{k=0}^{N-1} \sum_{j=1}^{N-1} v_{ik} v^{kj} \lambda_k^t,$$

where i is an arbitrary initial state, $V = (v_{ij})$ is the matrix of eigenvectors of P and $V^{-1} = (v^{ij})$ is its inverse. Since the coefficient of the largest eigenvalue $\lambda_0 = 1$ must be zero due to the fact that $P(\tau > t)$ goes to zero as $t \to \infty$, we can write

$$P_i(\tau > t) = \lambda_1^t \left[\sum_{j=1}^{N-1} v_{i1} v^{1j} + \sum_{k=2}^{N-1} \left(\sum_{j=1}^{N-1} v_{ik} v^{kj} \right) \left(\frac{\lambda_k}{\lambda_1} \right)^t \right]$$

$$\approx (\text{constant})\lambda_1^t$$

for large t, irrespective of the starting value i. In our case, λ_1 is the entry in the second position in the diagonal, namely $P_{11,}$ which is equal to q^{N-1}. In fact, all the eigenvalues can be found explicitly as $1, q^{N-1}, q^{2(N-2)}, q^{3(N-3)}, \ldots, q^{(N/2)^2}$ from largest to smallest. Therefore, we get

$$P\{D' > t\} \leqslant P\{\tau > t\}$$

$$\approx (\text{constant})\ q^{(N-1)t} \text{ for large } t,$$

where the first inequality follows from the fact that the delay of a retransmitted message is less than the time it takes all processes to receive that particular message and hence the time to bring the state of R to 0. As a result, the tail probability decays exponentially fast like that of a geometric distribution with parameter q^{N-1}. Note that geometric distribution is the discrete analogue of an exponential distribution. Both geometric and exponential distributions have light tails, whereas many statistics in network traffic have heavy-tails in the presence of long-range dependence and self-similarity. An exponential type marginal delay distribution and a Markovian recovery mechanism show that LRD is not expected for Bimodal Multicast.

4.2. Delay from simulations

We use the implementation of Bimodal Multicast formerly developed over ns-2 and the available ns-2 module of SRM in simulations. We compare SRM and Bimodal Multicast in the same simulation settings with the same sequence of random numbers. Initially, several independent runs of simulations were obtained to observe the effect of randomness in our results. For the statistical precision of our results for long-range dependence, each run lasts for 35,000 $\sim 2^{15}$ messages where each message is 210 bytes. With such a long sequence, independent runs with different seeds show almost no random variation in the estimated Hurst parameters and other statistics of performance. That is why the results are obtained from a single long stationary sequence of measurements for each parameter set. Our focus is on the scalability of each performance measure with respect to group size. The system wide message drop rate is set to 1% and higher drop rates are elaborated. The message rate seems to have no significant impact on the results. That is why it is fixed at 50 messages per second as a typical high-speed rate, unless stated otherwise.

Simulation scenario consists of transit-stub topologies with 40–120 nodes where every node is a group member. The sender is located on a central node and the receiver analyzed is located as far as possible on the network. The Internet can be viewed as a collection of interconnected routing domains where each domain can be classified as either a stub or a transit domain. Stub domains correspond to interconnected LANs and the transit domains model WAN or MANs [37]. We use gt-itm topology generator for producing

transit-stub topologies [38]. A certain drop rate is set on every link forming a system-wide noise. We vary two operating parameters, namely group size and system-wide noise rate. This scenario primarily focuses on the impact of randomized message loss over the traffic. We obtain our results from a sequence of 35,000 multicast data messages transmitted by the sender, and their timestamps logged at each receiver. This can be considered as a large file being multicast at constant bit rate to all receivers. We have reported in [12,13] that both protocols generate short-range dependent delays with H values around 0.5 up to the group size 80, but SRM delays show long-range dependence when the group size increases to 100 or more in these simulation settings.

In this section, we scrutinize the delays obtained from simulations for the aim of relating LRD characteristics to protocol recovery mechanisms. The delay histogram indicates that it is a mixture of two distributions, which are naturally the distributions of successful and recovered messages. The histograms of these for the largest group size $N = 120$ are given separately in Fig. 4 for Bimodal Multicast and in Fig. 5 for SRM. The delay of the messages transmitted successfully in the network shows almost no variation in the case of Bimodal Multicast in Fig. 4(a), and only a small portion of the messages have delays greater than 0.02 s. The recovered messages, which are relatively few in comparison to successful multicast messages, follow approximately an exponential distribution consistent with theoretical analysis above as shown in Fig. 4(b). The successful messages are transmitted almost with no random variation as in Fig. 4(a) may be due to the fact that the recovered messages have no adverse effect on the randomness in the network. On the contrary, delay of successful messages in the case of SRM being affected by the uncertainty in the network follow a normal distribution as shown in Fig. 5(a). The recovered messages follow a heavy right-tailed distribution as shown in Fig. 5(b).

To check if LRD originates from the recovered messages, hence the loss recovery mechanism of a protocol, we have estimated H from the delay of only recovered messages. The results are shown in Fig. 6. Indeed, the recovered messages for SRM show LRD for group sizes over 100. Bimodal Multicast generates random delays for recovered messages, but certainly in a short-range dependent manner with H around 0.5. We have estimated H using the delay of successful messages for SRM as well. Also successful messages show self-similar scaling with LRD in the case of SRM for $N = 100$ and $N = 120$ where H is 0.778 with

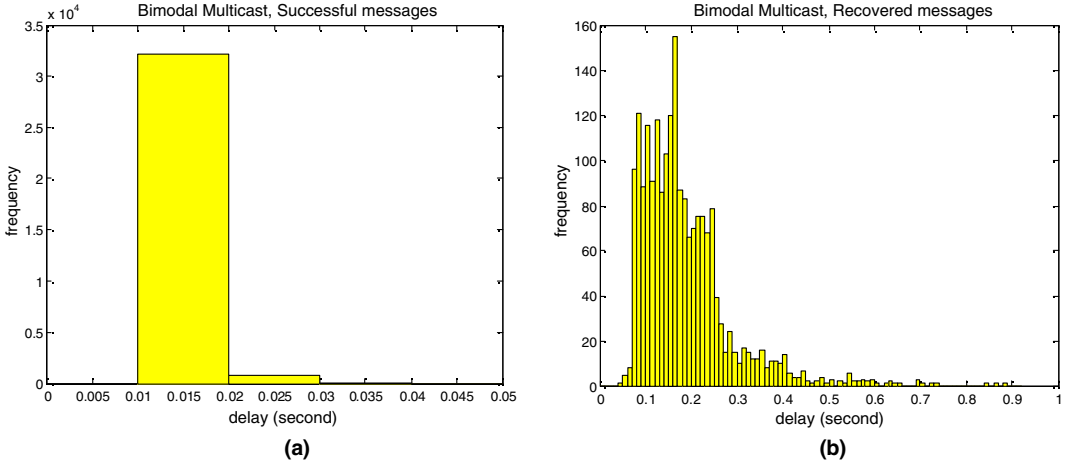

Fig. 4. Delay distribution for the farthest receiver in a group of size 120 in the case of Bimodal Multicast. (a) Successful messages and (b) recovered messages.

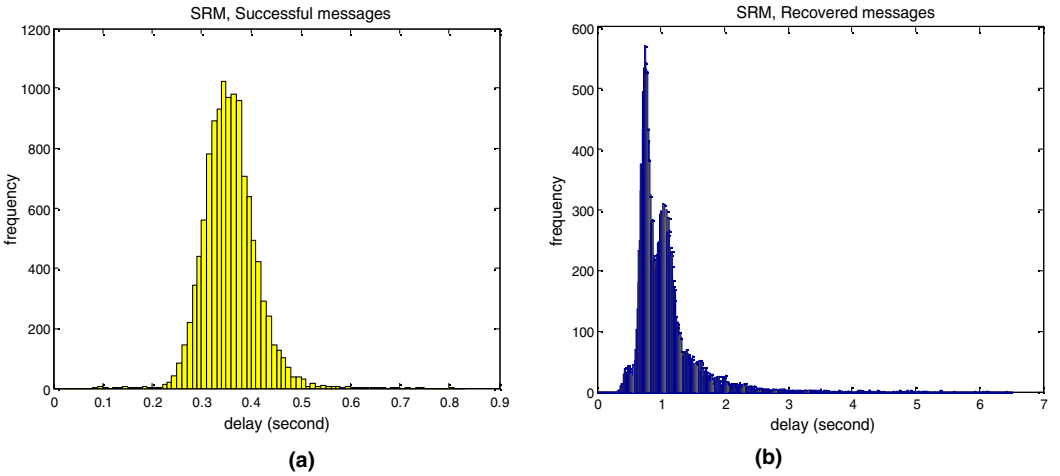

Fig. 5. Delay distribution for the farthest receiver in a group of size 120 in the case of SRM. (a) Successful messages and (b) recovered messages.

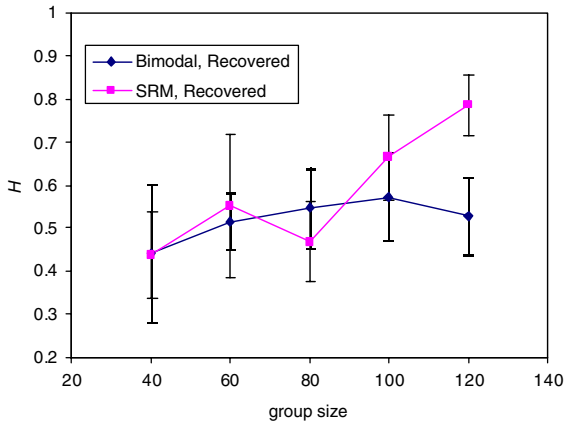

Fig. 6. Hurst parameter of delay versus group size for Bimodal Multicast and SRM for recovered messages.

a 95% confidence interval [0.693, 0.863] and 0.754 with a 95% confidence interval [0.685, 0.824], respectively.

It is striking that a transport level mechanism can induce self-similarity and LRD in the message delay sequence. The mean delay, a first order measure, increases linearly at a constant rate until group size 100, then picks up at $N = 120$ with a sharper increase, which is not shown here. On the other hand, LRD which is characterized through second order properties, namely correlations, appears at $N = 100$ and is sustained at $N = 120$. The scaling diagrams for recovered messages are similar to those for the complete delay sequence that are reported in [13]. As the group size increases from 100 to 120, the small time scaling becomes linear rather than nonlinear. This difference is very similar to the difference in the graphs of only TELNET and FTP traffic of 1990 Bellcore traces and 1994 Bellcore traces, respectively. In [4], this difference has been attributed to the increasing WWW traffic from 0% to 10% in 4 years, that is, to the application types. In our case, it is due to increasing group size and directly affected by the protocol [13]. The pattern change occurs at octave 6 in the scaling diagram, corresponding to about $2^6 = 64$ messages, that is, about the order of 1 s in view of the message rate 50 per second. This is in accordance with the results of TCP traffic examined in [4]. The smaller time scales might represent the effect of SRM's control actions at the granularity of time-to-live, and request and repair timers (in analogy to RTT and retransmission timer in the case of TCP), spanning time scales from 0.04 to 1 s. In contrast, the larger scales show the propagated effect of the protocol mechanism on the network due to congestion. Although simulated delay sequences span over an hour (up to octave 15), the last octaves have not been considered to ensure a reliable Hurst parameter estimation. As a result, LRD detected from the larger scales

spanning 1 s to a minute is a consequence of the transport protocol, as application/user level causes are absent in our simulations and the source is constant bit rate (CBR).

The scalability of Bimodal Multicast is remarkable at almost no cost in reliability. There are at most 1 or 2 messages lost among 35,000 messages in a run. The Hurst parameter is very stable in response to the increase of the group size. SRM makes utmost effort for reliability as no losses have been encountered in our simulations. This comes at a cost of longer delays and more importantly self-similar traffic patterns.

4.3. Comparison of analytical and simulation results for bimodal multicast

For a numerical comparison of our analytical upper bounds with simulations, we compute ε using the simulation settings above where every link has a fixed drop rate δ. Let the receiver be n hops away from the sender. Then the probability that there will not be a loss in any of the n links is $(1-\delta)^n$ and the probability of a message loss on this path is $\varepsilon = 1-(1-\delta)^n$. Taking n to be as large as possible in a given configuration would yield a pessimistic estimate of ε.

In Fig. 7(a) and (b), the upper bounds q^t and $q^{(N-1)t}$ are plotted with $q = 1-\beta(1-\varepsilon)^3$ for $N = 120$. Accordingly, the values of the parameters are as follows. The fanout probability $\beta = 1/120$ is found by the uniform choice of a single member of the group at each gossip stage. The maximum number of hops n is 6, and the constant drop rate at each link is $\delta = 1\%$. As a result, the failure probability q is computed to be 0.9926. The bound q^t turns out to be a very loose bound when we plot it together with the empirical estimate of $P\{D^t > t\}$ from simulated delay sequence in Fig. 7. On the other hand, the bound $q^{(N-1)t}$ is strict enough for the tail probabilities. Indeed, the tail of the empirical distribution decays exponentially fast.

5. Traffic at the link level

The initial identification of long-range dependence and self-similarity in the network has been through extensive analysis of traffic at the link level [1]. Numerous studies have verified this result through traffic counts, and some have analyzed delay and interarrivals for LRD as related statistics [2]. However, physical models, which explain LRD are devised only for traffic counts [3]. If LRD is detected at the link level, its implications such as buffer provisioning, link speeds, and in general, queuing performance are clear [39,40].

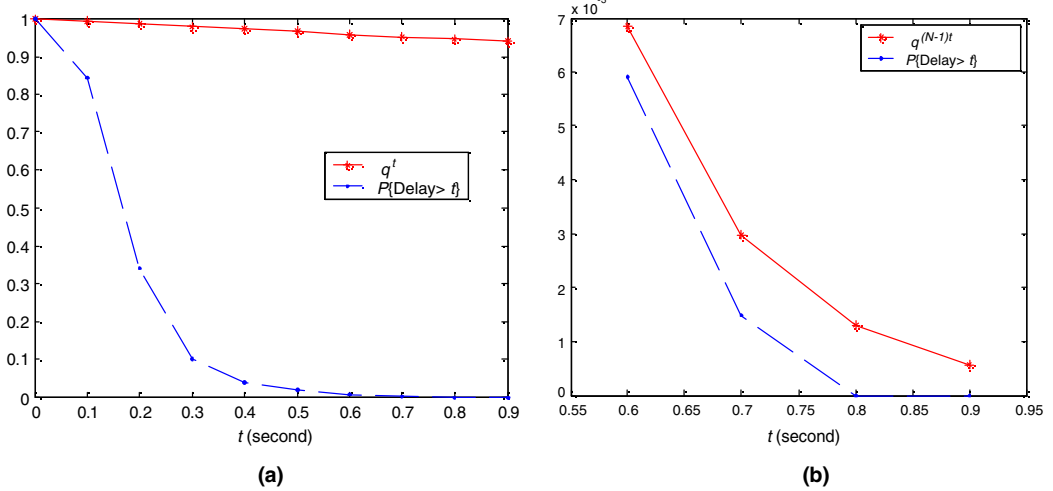

Fig. 7. Empirical complementary probability $P\{D^t > t\}$ and the upper bounds. (a) q^t and (b) $q^{(N-1)t}$ versus time t for $N = 120$.

That is why self-similarity characteristics of the traffic generated by a transport protocol can be conclusive only after the study of the link level traffic. In this section, we study traffic counts from simulations and complete the statistical picture with an analysis of interarrival distributions.

Delay has been studied by itself as an important performance measure in previous work [12,13], the predictions of which are substantiated with further analysis in the present study. As a matter of fact, the delay distribution that we have established in Section 4 can be considered as mainly queuing delay, which is a result of the link level counting process. The delay of a message between a sender-receiver pair in the network can be interpreted as the total delay of tandem queues along its route [34]. Since queuing behavior is determined by the traffic counts, the presence or absence of LRD for delay gives only an indirect indication for the link level, which we analyze next.

5.1. Traffic counts

At the link level, we analyze the number of messages addressed to a fixed receiver in the network from simulations. This constitutes the sequence of traffic counts per time unit, which are data and overhead messages. The simulation settings are the same as in Section 4 and the traffic between the sender and receiver pair is now considered at the link level. Since the messages are sent at a rate of 50 per second, tracing them at 200 ms. intervals yields a sufficient resolution. Physically, the traffic stream does not flow over a single link, but it is aggregated from a few incoming links to the receiver and is worth characterizing for comparison with the delay properties studied for the same receiver.

The mean number of messages per second and the Hurst parameter obtained from traffic counts addressed to a fixed receiver are given in Fig. 8. The stress on the network can be observed at group size 120 for both mean traffic and the Hurst parameter for SRM. For $N = 100$, the traffic counts are short-range dependent in contrast to corresponding delay sequence. In any case, Bimodal Multicast is not affected by the increase of N and it generates short-range dependent traffic counts.

The traffic count sequences addressed to a fixed receiver for $N = 120$ are plotted in Fig. 9(a) and (b) for Bimodal Multicast and SRM, respectively. The beginning 20 s of the SRM sequence looks nonstationary, which we exclude from analysis while estimating the Hurst parameter. The bursty behavior of SRM is clear. On the other hand, the traffic generated by each protocol at a single link has direct implications on traffic engineering such as buffer and link capacity provisioning. That is why we have monitored a single link connecting

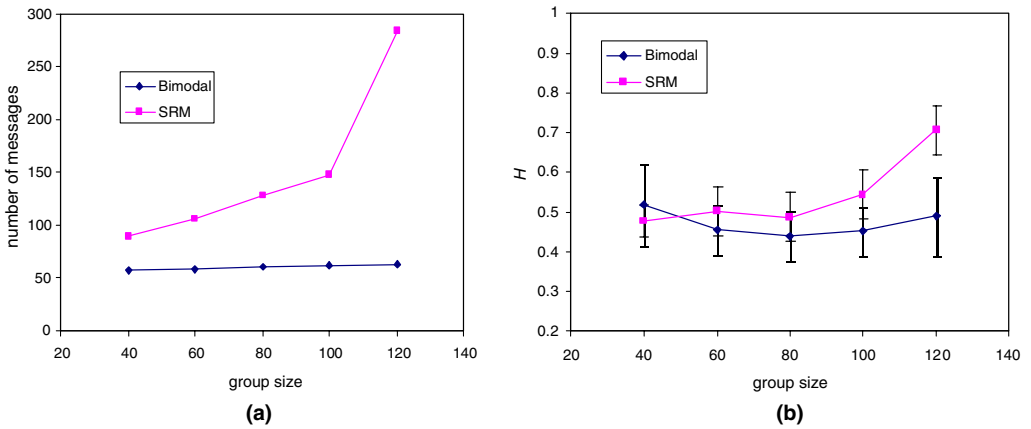

Fig. 8. (a) Mean (per second) and (b) Hurst parameter of the traffic counts versus the group size at a receiver for Bimodal Multicast and SRM.

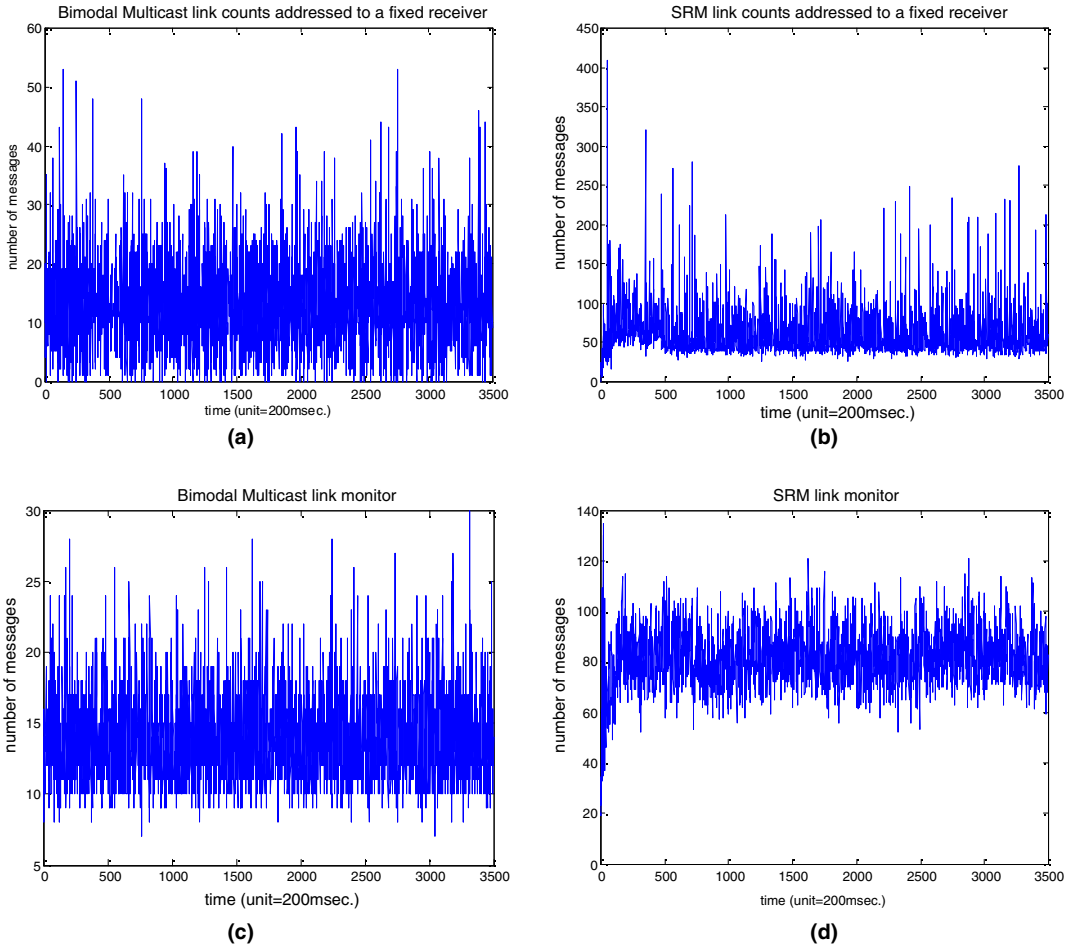

Fig. 9. Sequence of link counts.

to the same fixed receiver for all traffic going through it for a duration of about 700 s. The traffic sequences analyzed for Bimodal Multicast and SRM for $N = 120$ are given in Fig. 9(c) and (d), respectively. We see that LRD is sustained, as H values are qualitatively similar to those plotted in Fig. 6 with the same octaves corresponding to the same time scales. This is due to the fact that it takes 700 s for 35,000 messages to be sent in view of the sending rate of 50 per second. The exact H values are reported elsewhere [41] for comparison purposes. Here, we show that the link level traffic for SRM also has a rich scaling as ubiquitously found in the Internet traffic. It is almost exactly self-similar [14] due to a linear scaling diagram over almost all octaves for the cumulative counts given in Fig. 10(a). In parallel to this observation, the plot of multiscale diagram [42] given in Fig. 10(b) is almost linear in the moments q. If it was exactly linear, the traffic counts could be identified as monofractal. Slight nonlinearity indicates that it could be a multifractal process. In the Internet, multifractality is attributed to TCP's control of window size, which has a multiplicative behavior. Although SRM does not have such a congestion control, its timing mechanism works similar to TCP. The protocol actions yield a fractal behavior at all scales in view of log-scale diagrams for several moments, which are not shown here.

An H value of 0.5 for Bimodal Multicast indicates independence of the increments of traffic

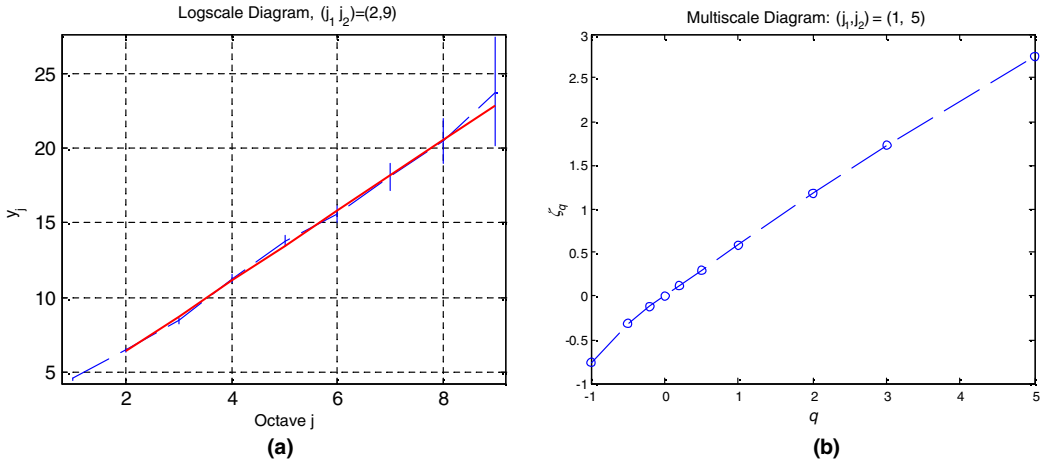

Fig. 10. (a) Logscale and (b) multiscaling diagram of SRM cumulative link counts.

counts plotted in Fig. 9(a) and (c). Poisson process or Brownian motion can model the cumulative process obtained from these counts. For the cumulative of SRM traffic counts given in Fig. 9(d), a fractional Brownian motion could be a good fit. This is a strictly self-similar, monofractal model with long-range dependent increments and a symmetric, namely normal, marginal distribution. On the other hand, the distribution of traffic counts in Fig. 9(c) is skewed. A stable process with long-range dependence having non-Gaussian marginals could fit well in this case. Hence, we have established the properties of LRD and self-similarity for the traffic generated by SRM and short-range dependence for Bimodal Multicast, as predicted by the delay distributions and recovery mechanisms studied in the previous section.

The anti-entropy protocol of Bimodal Multicast uses gossiping, which is a spatial mechanism in contrast to temporal timer mechanism of SRM. Resembling TCP that adaptively sets timers or congestion control windows, SRM algorithms dynamically adjust their control parameters based on the observed performance within a multicast session. The adaptive nature and the window mechanism of TCP are discussed in [43] as a means of generating self-similarity. This helps explaining the difference in the traffic patterns. Temporal behavior such as heavy-tailed session durations (as a result of user behavior, like off times, or heavy-tailed file size distributions) directly translates to long-range dependence. In the case of Bimodal Multicast, the burden is distributed spatially by the gossiping mechanism, which results in a Markovian temporal structure. Markov dependence in time is much weaker and hence does not lead to LRD. See [44] for a similar space versus time stretching analogy established for UDP and TCP, respectively. UDP shows less self-similar characteristic due to lack of reliability compared to TCP. On the other hand, Bimodal Multicast provides high level of probabilistic reliability guarantees as well as producing short-range dependent traffic. In SRM, a process multicasts request message to the whole group when it detects a message loss in order to guarantee reliable delivery. Request and repair timers are exploited to suppress duplicate requests and repairs for the same message loss. A corresponding repair message in response to a request is also in the form of multicast to the whole group. This feature of SRM's loss recovery mechanism makes its background overhead and bandwidth requirements to increase as a function of group size. As a result, there is zero loss in our simulations but at the expense of self-similar traffic with long-range dependence. The delays are high, loss recovery mechanism works, but imposes a self-similar pattern that implies low performance.

5.2. Interarrival distributions

The interarrival distributions reflect the performance implications of the traffic patterns from another point of view. For example, message interarrival distribution of a protocol is related to its throughput stability. As discussed in [9], throughput stability is a critical requirement for several distributed applications. Our simulations show that the interarrival distribution of only the data messages is approximately normally distributed when the network is not pressured. This is true for Bimodal Multicast in all cases and for SRM in smaller group sizes up to 100. For SRM, as the group size increases, the distribution becomes more right skewed (long right tail) and ultimately an exponential distribution fits well at $N = 120$. This is verified with a probability plot, which is not shown here. Although an exponential interarrival distribution is associated with short-range dependence, in particular a Poisson process, such a model would be applicable to data messages only. When overhead messages are included in addition to data messages, the total link traffic is long-range dependent for SRM as reported in Fig. 8(b). The means of the distributions also increase as the skewness gets more pronounced. Basically, the means are around 20 ms. as the message multicast rate is 50 per second. The standard deviation increases gradually in SRM to 0.0217, whereas it is stable for Bimodal Multicast around 0.006.

We also scrutinize the interarrival distribution at a single link as it is relevant for performance prediction such as buffer overflow probabilities. We obtain the interarrival sequences from the monitored link. In this case, the mean and standard deviation of interarrivals are not comparable for Bimodal Multicast and SRM because the first has a lower amount of overhead traffic whereas the latter suffers from excessive overhead for $N = 120$. However, SRM having a higher standard deviation of 3.752 ms. than its mean, namely 2.458 ms, is much more right skewed than Bimodal Multicast which has a mean of 13.558 ms and a standard deviation of 9.898 ms. A proper probability plot is harder to obtain in this case, as the link monitor module of ns-2 reports the timestamps with a fixed number of significant digits not decimal places by default. So, some of the distinct, especially smaller, interarrival times are aliased to be the same by round off. Nevertheless, we provide a Weibull probability plot in Fig. 11 in order to illustrate that the tail of the distribution is heavier than exponential. For larger quantiles of the Weibull distribution given in y-axis, we see a linear alignment in the probability plot when aliasing around 10^{-3} and 10^{-2} seconds are ignored. This is not observed in an exponential probability plot. Besides, a Pareto probability plot shows that the tails are not as heavy as coming from a Pareto distribution. This is an approximate analysis due to aliasing, but consistent with LRD identified from traffic counts. Note that the analysis of traffic counts is not affected by the round off in the time stamps because the time unit 200 ms is coarse enough compared to the interarrivals given in the x-axis of Fig. 11. Nevertheless, this resolution is sufficient for the scaling analysis.

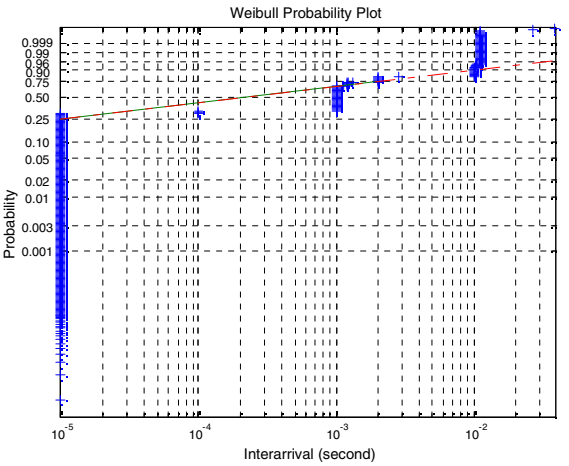

Fig. 11. Probability plot for interarrivals of SRM's link monitor, $N = 120$.

6. Performance measures and effect of topology

In order to link the traffic behavior to the protocol recovery mechanisms, we study other

performance measures, namely throughput, overhead and duplicates, as well as effects of system-wide drop rate and network topology on traffic characteristics in this section.

6.1. Throughput, overhead and duplicates

We report throughput, mean number of data messages received per second, and the overhead messages received per second given in Fig. 12(a) and (b), respectively. Note that the throughput is expected to be 50 due to the message multicast rate at the sender. Similar to the mean delay, the throughput decreases and the overhead increases sharply at $N = 120$ for SRM whereas both are scalable for Bimodal Multicast. Besides, although the mean throughput is the same, the variance is significantly smaller for Bimodal Multicast for smaller group sizes, not shown here. The behavior of the overhead until $N = 100$ has been documented in [9,45] indicating that the increase is linear for SRM. We have hence detected that the performance fades further for $N = 120$ although LRD starts even earlier at $N = 100$ at the 1% system wide drop rate. The number of duplicate messages received per each data message is shown in Fig. 13 which also demonstrates that Bimodal Multicast is scalable. For SRM the behavior is in accordance with that of the mean delay rather than the Hurst parameter; there is a significant change after $N = 100$.

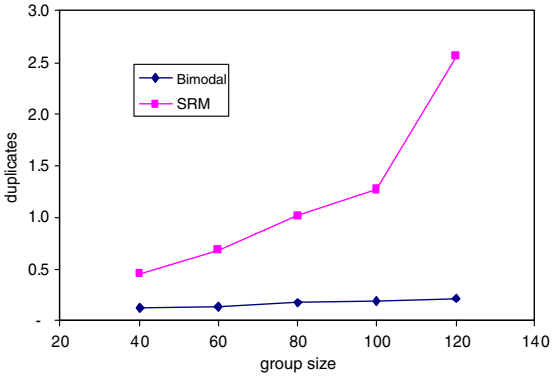

Fig. 13. Duplicates per each data message versus group size for Bimodal Multicast and SRM.

6.2. Effect of system-wide drop rate

We have also run simulations with higher system wide drop rates, namely 2%, 5% and 10% at each link. The results are similar to 1% case. In particular, the initial analysis of [12,13] includes 2% comparatively with 1%. As an adverse effect at 10% system wide drop rate, the interarrival distribution is exponential also for Bimodal Multicast. Otherwise, Bimodal Multicast's performance is scalable with high drop rates as well. SRM's performance decreases until $N = 100$ gradually, thereafter sharply. Surprisingly, at higher rates 5% and 10%, SRM delay does not show LRD at $N = 100$, but only for $N = 120$. The sharp increase in the mean delay and decrease in throughput also occur

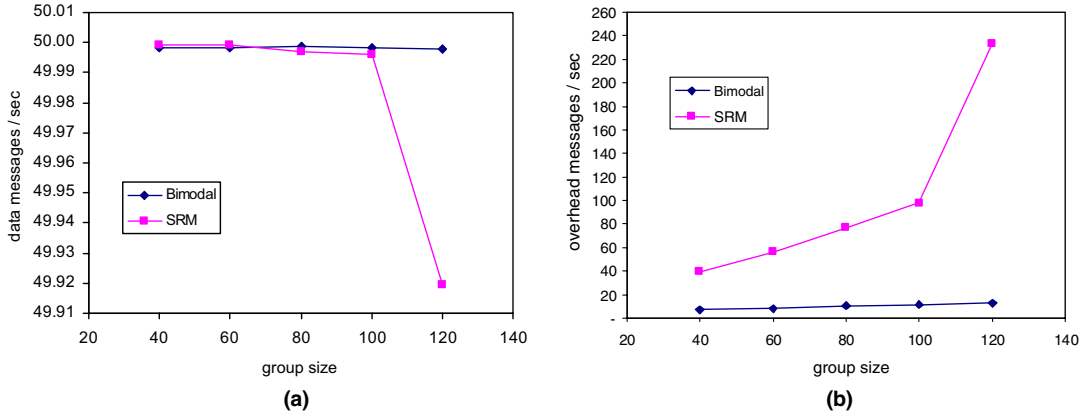

Fig. 12. (a) Throughput and (b) overhead versus group size for Bimodal Multicast and SRM.

at $N = 120$, similar to 1% and 2% cases. A possible explanation could be as follows. In general, LRD occurs due to the slow decay of the autocorrelation of delay. The bursts related to self-similarity may, in a sense, be prevented with higher drop rates. When a drop occurs, the message is to be recovered. By the time it is resent by a group member, the dependence structure of the consecutive messages is destroyed. A similar situation to high drop rates is small buffers leading to overflow of messages. In this case, H turns out to be relatively small [44]. Vice versa, larger buffers allow for more messages to be in-waiting and hence increase the dependence in the traffic and H.

Heterogeneous network characteristics such as different links having different drop rates can also be considered. The current results are likely to hold in that case as well, since quite a random loss rate arises between a sender and receiver through a random number of links in transit-stub topology. For example, three different random topologies have been considered in [13] for each group size and the results obtained are similar.

6.3. Effect of topology

In another scenario where clusters are connected by a bottleneck link, we study both the transport level delays and the link level traffic counts. Such multicluster topologies might be considered as local area networks connected by long distance links where routers with limited bandwidth connect group members. We simulate a clustered network with variable size consisting of two fully connected clusters, and a single link connects those clusters. All nodes are members of the multicast group among which there is one multicast sender. There is 1% intracluster noise formed in both clusters, and a varying high noise rate is injected on the link connecting the clusters which behaves as a bottleneck link. The sender and the receiver are located across clusters. Message rate is 100 messages per second, and the bottleneck link is monitored. Two different levels of bottleneck drop rate and group size are considered. The results are reported in Tables 1 and 2.

We do not observe LRD in either Bimodal Multicast or SRM in this topology. In comparison to previous topologies, the overhead is higher in Bimodal Multicast because the gossip rate in this case is taken to be twice every 100 ms rather than once. This is needed as buffer overflows occur in this setting. Consequently, the delays are lower for Bimodal Multicast. Throughput decreases slightly with higher drop rate at the bottleneck, but is not affected by the increasing group size in Bimodal Multicast. In SRM, it decreases significantly with the increase of bottleneck noise or group size. All the interarrival distributions are exponential. We have observed that even Bimodal Multicast, in addition to SRM, generates exponential interarrivals when the drop rate is as high as 10% for all group sizes. Here, the high bottleneck noise might be the reason for a skewed interarrival distribution.

We have in fact also considered larger group sizes for both topologies. In the version of ns-2 used in this study, the simulations do not take some of the queuing delays into account for group sizes larger than 128. Delay streams truncated in this manner produce better performance mistakenly, and hence are not comparable to the results here. If a cluster size could be increased to 100 or 120 without affecting the simulation approach,

Table 1
Hurst parameter and performance measures in clusters—Bimodal Multicast

Drop rate (%)	N	Link level (messages)				Transport level (delay in seconds)				Performance		
		Mean	Std. Dev.	H	95% CI	Mean	Std. Dev.	H	95% CI	Loss ratio	Throughput	Interarrival
25	60	701	240	0.528	[0.466, 0.590]	0.057	0.064	0.552	[0.536, 0.568]	2.857E−05	99.9857	Exp(0.01)
50	60	786	221	0.495	[0.433, 0.557]	0.122	0.111	0.534	[0.518, 0.550]	3.43E−04	99.9171	Exp(0.01)
25	120	1309	332	0.511	[0.449, 0.573]	0.0674	0.0668	0.572	[0.556, 0.588]	8.571E−05	99.9657	Exp(0.01)
50	120	1400	361	0.550	[0.488, 0.612]	0.120	0.102	0.570	[0.554, 0.586]	1.71E−04	99.9600	Exp(0.01)

Table 2
Hurst parameter and performance measures in clusters—SRM

Drop rate (%)	N	Link level (messages)				Transport level (delay in seconds)				Performance		
		Mean	Std. Dev.	H	95% CI	Mean	Std. Dev.	H	95% CI	Loss ratio	Throughput	Interarrival
25	60	404	218	0.529	[0.467, 0.591]	0.066	0.137	0.481	[0.464, 0.497]	0	99.9829	Exp(0.01)
50	60	368	162	0.585	[0.486, 0.684]	0.226	0.744	0.490	[0.474, 0.506]	5.714E−05	99.1445	Exp(0.01)
25	120	547	257	0.499	[0.399, 0.598]	0.191	0.252	0.585	[0.569, 0.602]	0	99.7151	Exp(0.01)
50	120	421	190	0.557	[0.458, 0.657]	0.237	0.704	0.513	[0.497, 0.529]	5.714E−05	99.1445	Exp(0.01)

the topology would be comparable to transit stub in each cluster. In this case, we would expect LRD for SRM. For present settings of cluster topology, the bottleneck link having a high noise rate causes packet drops and may have destroyed the correlation structure. This is similar to the effect of high system-wide noise rate for transit-stub topology. We conclude that the topology is a factor in traffic behavior when combined with the size of the network.

7. Self-similar background traffic

In order to detect the interaction of multicast traffic with the existing self-similar traffic, we generate background traffic via multiple long-lived TCP flows during simulations. In particular, a total of 30 on/off sources send TCP packets to 30 other receivers on group sizes varying from 60 to 120. It is well known that when sufficiently many of traffic streams from such sources are aggregated, LRD arises at the link level [46]. We sample on and off times from a Pareto distribution with shape parameter $\alpha = 1.5$ and mean 500 ms each. In order to make sure that self-similar background traffic is obtained when there is no multicast traffic, we monitor an inner link on the network and estimate the Hurst parameter. The result is depicted in Fig. 14(a) as *Background* series. The Hurst parameter varies around 0.7 for all group sizes indicating LRD. This is consistent with the on/off source model of data traffic where H is predicted to be $(3 - \alpha)/2 = 0.75$.

After detecting the link that carries self-similar traffic, we monitor it again this time superimposing multicast and TCP traffic flows on the same network. Fig. 15(a) shows Hurst estimates from three link counts in this case, simultaneously with the

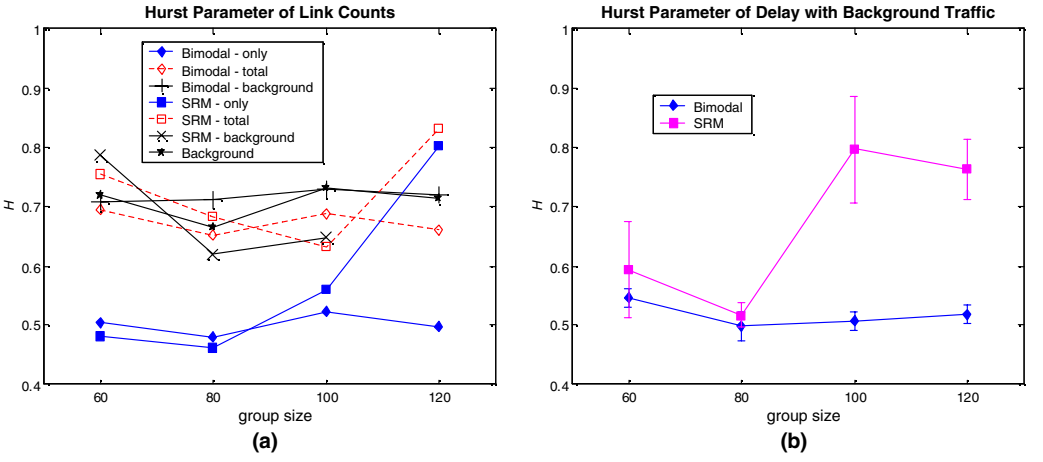

Fig. 14. Hurst parameter of (a) link counts and (b) delay with background traffic.

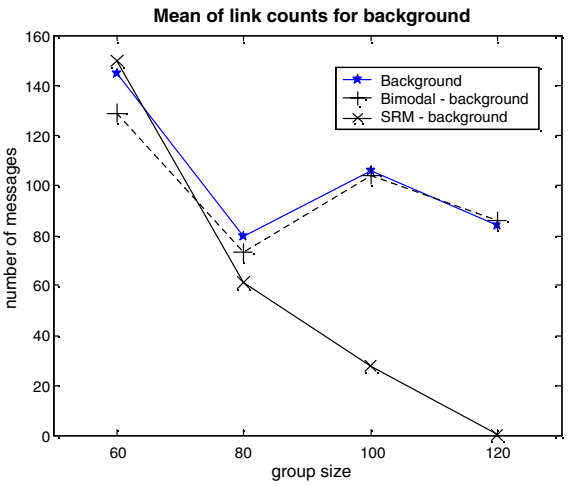

Fig. 15. Mean of link counts for background traffic vs group size.

TCP traffic stream indicated as *Background* above. *Bimodal-total* and *SRM-total* refer to total link counts from the monitored link and hence include both multicast and background traffic. The characteristics of each of the multicast streams (denoted as *Bimodal-only* and *SRM-only*) as well as background streams (denoted as *Bimodal-background* and *SRM-background*) are also established through their Hurst parameters. When we compare the three estimates, namely, total, only and background for each protocol, we see that Bimodal Multicast neither restricts nor gets affected by the background traffic. Hurst estimates of *Bimodal-only* are all around 0.5 indicating short range dependence as in Fig. 8(b). Similarly, Hurst estimates of the background traffic accompanying Bimodal Multicast (*Bimodal-background*) are also very close to those estimates obtained from *Background*. There is a slight, but not significant difference only for $N = 80$. The Hurst estimates of the total traffic are between these background and protocol only values. As a result, the total traffic is well behaved in terms of LRD with the addition of Bimodal Multicast to the self-similar background traffic. In Fig. 14(b), Hurst parameters estimated from delay sequence are given. Bimodal Multicast generates short range dependent traffic for all group sizes and SRM streams yield similar Hurst parameters as in Fig. 6.

SRM itself remains unaffected by the background traffic, but has an adverse effect on it at the link level. The Hurst parameters as depicted in Fig. 14(a) are low in *SRM-only* streams for group sizes up to 100, but indicates LRD for $N = 120$ as in Fig. 8(b). For $N = 120$, the monitored link carries only a negligible amount of background traffic. That is why it is not possible to estimate H for background traffic in this group size. In fact, as the group size increases, less and less background traffic is carried over the monitored link compared to earlier background measurements, as shown in Fig. 15. This behavior might be due to the rerouting of TCP streams or the activation of TCP congestion control in response to SRM traffic.

8. Self-similar sources and strict self-similarity

We have characterized the traffic generated by two multicast protocols in the isolated case when only multicast communication takes place and also when self-similar background traffic is present in the same networking environment. In both cases, the sender is assumed to multicast at a constant bit rate. However, when the network is congested and flow control is imposed, the multicast sender can behave like a self-similar source although constant bit rate is aimed. In this section, we characterize the traffic generated by SRM for larger group sizes 100 and 120 with a self-similar source. This is an exact solution replacing the preliminary results about the larger group sizes reported elsewhere [41,47]. We put the self-similar behavior of SRM in theoretical perspective with respect to the previous sections.

We have shown in [41] that when a self-similar source, namely an on/off sender that transmits with Pareto on and off times, is considered, traffic becomes worse for SRM in terms of both transport delays and at the link level. On the other hand, Bimodal Multicast generates desirable delays; however long-range dependence arises in the link level due to on/off source as expected. The Hurst parameter of link counts is consistent with the shape parameter of the on/off source. Bimodal

Multicast translates the self-similar behavior at the source to the link level with no further addition.

For $N = 100$ and 120 in SRM, we have simply reported $H = 1$ as the log-scale diagram yields an H value greater than 1 for both the delay sequence over the network and the traffic counts at the link. This is in view of the fact that H must take values in $(0.5, 1)$ in presence of LRD. Since the estimates do not fall into $(0.5, 1)$, we see that the traffic does not behave like a process with LRD. However, there is no reason to suspect nonstationarity for the increments of traffic as the other performance measures are quite stationary, and more concretely, log-scale diagrams from partitions of the sequence show similar characteristics. Strict self-similarity may occur with or without LRD [14]. It can be characterized through the cumulative process, namely cumulative traffic counts over time as we have already done for the link counts with a CBR source. The main difference here is that H is now greater than 1, which indicates that an infinite variance self-similar process can adequately describe the traffic. Although used in previous sections, the logscale diagram [15] which is based on second moments may not be used in this case. Due to the indication of infinite variance, a scaling diagram especially devised for infinite variance stable processes is given in Fig. 16, which is a result of our implementation of the estimation method described in [16]. The variable y is different from the logscale diagram and the slope yields $H + 1/2$. As a result, Fig. 16 which is obtained from the cumulative traffic counts of SRM for $N = 120$ yields $H = 1.1$, a value slightly larger than 1. The only self-similar stable process with $H > 1$ is α-stable Levy motion. On the other hand, if only the mid-octaves of 5–10 are used in the estimation due to concerns described in [16], we get $H = 0.78$, but under the assumption of infinite variance. A linear fractional stable motion is such a stochastic process. It shows long-range statistical dependence, which is like LRD but has a different definition due to infiniteness of second moments. For our purposes, the implications of infinite variance is more important than the exact value of the self-similarity parameter H because in that case, the queuing behavior at a link is expected to be worse than self-similarity with LRD. For a comparison of queuing implications of FBM, which is a self-similar model with LRD, and α-stable Levy motion, which is a model with infinite variance, see [48]. Hence, the characterization of the stochastic process that can model the traffic generated by SRM provides us with the prediction of performance. When going from a CBR to on/off source, we see that performance degrades even further. From stochastic modeling point of view, it is also interesting that SRM yields almost all important models of self-similarity under various scenarios.

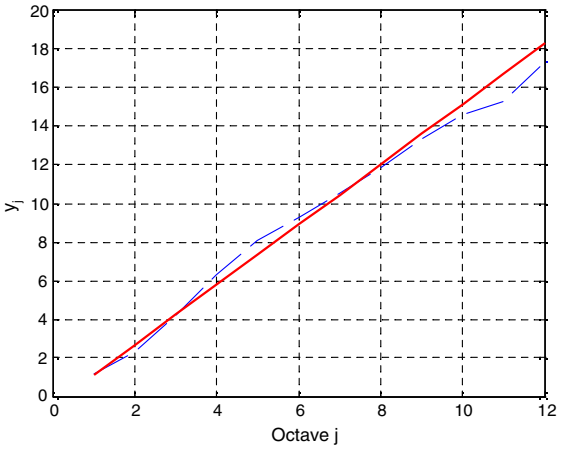

Fig. 16. Scaling diagram of SRM cumulative link counts with an on/off source, for estimation of H of an α-stable process.

9. Conclusion

This article focuses on traffic characterization of transport level reliable multicasting, and contributes to identifying better protocol components for multicast transport. In particular, we concentrate on two scalable and reliable multicast protocols as case studies, namely Bimodal Multicast and SRM, and analyze the traffic generated by them through extensive simulations and theoretical work. We have analyzed the protocols first under a CBR source to isolate the traffic that they generate, and also in realistic network environments, namely in the presence of background traffic, and separately when the source is self-similar. This article conclusively studies the link level traffic,

substantiates delay characteristics with precise theoretical analysis, studies background traffic, and compares with the case of self-similar sources for which theoretical characterization of SRM traffic is accomplished as an extension of preliminary work.

Bimodal Multicast is based on peer-to-peer epidemic paradigm for loss recovery. If a process detects a message loss in the end of a gossip round, it requires a unicast request and repair message to recover the loss. Bimodal's background overhead is scalable and does not increase with the group size. We have analyzed the marginal delay distribution for Bimodal Multicast and shown that it decays exponentially. This substantiates that LRD is not expected intrinsically due to the Markovian character of the protocol. Hence, its traffic does not manifest self-similarity with long-range dependence in the absence of application level causes, namely under a CBR source.

The same load is offered to the network, but the resulting traffic patterns are different with the two reliable multicast protocols. We have shown empirically that long-range dependence can be induced by transport level. SRM traffic at the link level becomes long-range dependent with $H > 0.7$ when the group size is over 100–120 in our settings, which is common to many current distributed applications. While long-range dependence is induced on the network traffic at large time scales, the link level traffic has a fractal characteristic spanning almost all scales. SRM's having a similar loss recovery mechanism to TCP implies that ubiquitous presence of self-similarity in data networks might be due to wide spread availability of TCP. Although we have not proven how exactly the timing mechanism of SRM shapes a self-similar traffic at the link level, we have identified several instances where various theoretical models of self-similar traffic are applicable. Such an identification has been useful for the prediction of network performance under such a transport protocol. As future work, the distribution of time-out parameters can be investigated for heavy-tails to figure out any causal relationship with LRD.

A concern in the deployment efforts of multicast model on large-scale is that it might flood the network. Bimodal Multicast discretely feeds well-behaved traffic and copes with the existing self-similarity. The epidemic mechanism facilitates this outcome due to its Markovian structure. In contrast, SRM suppresses the background flow and imposes self-similarity. Self-similar sources have even worse consequences on SRM. Because this time the traffic is an α-stable Levy motion and its queues decay even more slowly.

Acknowledgements

This work is partially supported by TUBITAK (The Scientific and Technical Research Council of Turkey) and COST (European Cooperation in the field of Scientific and Technical Research) Action 279 "Analysis and Design of Advanced Multiservice Networks supporting Mobility, Multimedia, and Internetworking".

References

[1] W.E. Leland, M.S. Taqqu, W. Willinger, D.V. Wilson, On the self-similar nature of ethernet traffic (Extended version), IEEE/ACM Transactions on Networking 2 (1) (1994) 1–15.

[2] W. Willinger, V. Paxon, R. Reidi, M. Taqqu, Long-range dependence and data network traffic, in: P. Doukhan, G. Oppenheim, M.S. Taqqu (Eds.), Long-range Dependence: Theory and Applications, Birkhauser, Basel, 2001.

[3] M. Çağlar, A Long-range dependent workload model for packet data traffic, Mathematics of Operations Research 29 (2004) 92–105.

[4] A. Feldmann, C. Gilbert, W. Willinger, T.G. Kurtz, The changing nature of network traffic: scaling phenomena, Computer Communication Review 28 (1998) 5–29.

[5] B. Sikdar, K. Vastola, On the contribution of TCP to the self-similarity of network traffic, in: Proceedings of the 2001 Tyrrhenian International Workshop on Digital Communications: Evolutionary Trends of the Internet, Taormina, Italy, 17–20 September 2001.

[6] K. Park, G.T. Kim, M.E. Crovella, On the effect of traffic self-similarity on network performance, in: Proceedings of the SPIE International Conference on Performance and Control of Network Systems, November 1997.

[7] J. Kilpi, A Portrait of a GPRS/GSM Session, in: Proceedings of the 18th International Teletraffic Congress, September 2003.

[8] K. Tutschku, P. Tran-Gia, A Traffic Profile of the eDonkey Filesharing Service, COST-279 Project, 279TD(03)049, 2003.

[9] K.P. Birman, M. Hayden, Ö. Özkasap, Z. Xiao, M. Budiu, Y. Minsky, Bimodal multicast, ACM Transactions on Computer Systems 17 (2) (1999) 41–88.
[10] S. Floyd, V. Jacobson, C. Liu, S. McCanne, L. Zhang, A reliable multicast framework for light-weight sessions and application level framing, IEEE/ACM Transactions on Networking 5 (6) (1997) 784–803.
[11] Ö. Özkasap, M. Çağlar, Multicast network traffic and long-range dependence, in: Proceedings, IASTED, International Conference on Advances in Communications, Rhodes, Greece, July 2001.
[12] Ö. Özkasap, M. Çağlar, Network traffic properties of bimodal multicast protocol, Turkish Journal of Electrical Engineering & Computer Sciences 11 (1) (2003) 17–34.
[13] Ö. Özkasap, M. Çağlar, Traffic behavior of scalable multicast: self-similarity and protocol dependence, in: Proceedings of the 18th International Teletraffic Congress, September 2003.
[14] P. Abry et al., Wavelets for the analysis, estimation, and synthesis of scaling data, in: K. Park, W. Willinger (Eds.), Self-Similar Network Traffic and Performance Evaluation, Wiley, New York, 2000.
[15] D. Veitch, P. Abry, A wavelet based joint estimator of the parameters of long-range dependence, IEEE Transactions on Information Theory 45 (1999) 878–897.
[16] P. Abry, M.S. Taqqu, B. Pesquet-Popescu, Wavelet based estimators for self-similar α-stable processes, International Conference on Signal Processing (ICSP), IFIP 16th World Computer Congress, 2000.
[17] L.A. Kulkarni, S.Q. Li, Traffic modeling: matching the power spectrum and distribution, GLOBECOM '95, IEEE 3 (1995) 1701–1706.
[18] D.P. Heyman, T.V. Lakshman, What are the implications of long-range dependence for VBR-video traffic engineering, IEEE/ACM Transactions on Networking 4 (1996) 301–317.
[19] T.J. Lee, G. de Veciana, Model and performance evaluation for multiservice network link supporting ABR and CBR services, IEEE Communications Letters 4 (2000) 375–377.
[20] A. Sang, S.Q. Li, A predictability analysis of network traffic, INFOCOM 2000, IEEE 1 (2000) 342–351.
[21] D.P. Heyman, D. Lucantoni, Modeling multiple IP traffic streams with rate limits, IEEE-ACM Transactions on Networking 11 (2003) 948–958.
[22] M. van Foreest, M. Mandjes, W. Scheinhardt, Analysis of a feedback fluid model for heterogeneous TCP sources, Stochastic Models 19 (2003) 299–324.
[23] A. Demers, D. Greene, C. Hauser, W. Irish, J. Larson, S. Shenker, H. Sturgis, D. Swinehart, D. Terry, Epidemic algorithms for replicated database maintenance, in: Proceedings of the Sixth ACM Symposium on Principles of Distributed Computing, British Columbia, Vancouver, 1987, pp. 1–12.
[24] K. Lidl, J. Osborne, J. Malcome, Drinking from the firehose: Multicast USENET news, USENIX Winter 1994, pp. 33–45.
[25] R. Ladin, B. Lishov, L. Shrira, S. Ghemawat, Providing availability using lazy replication, ACM Transactions on Computer Systems 10 (4) (1992) 360–391.
[26] S. Bajaj, L. Breslau, D. Estrin, et al., Improving simulation for network research, USC Computer Science Dept. Technical Report 99-702, 1999.
[27] J. Gemmell, T. Montgomery, T. Speakman, N. Bhaskar, J. Crowcroft, The PGM reliable multicast protocol, IEEE Network (January/February) (2003).
[28] S. Paul, K. Sabnani, J.C. Lin, S. Bhattacharyya, Reliable multicast transport protocol (RMTP), IEEE Journal on Selected Areas in Communications, Network Support for Multipoint Communication (special issue) 15 (3) (1997).
[29] A.S. Tanenbaum, M. van Steen, Distributed Systems: Principles and Paradigms, Prentice Hall, 2002, ISBN 0-13-088893-1.
[30] C. Labovitz, G.R. Malan, F. Jahanian, Internet routing instability, in: Proceedings of SIGCOMM '97, 1997, pp. 115–126.
[31] V. Paxson, End-to-end internet packet dynamics, in: Proceedings of SIGCOMM '97, 1997, pp. 139–154.
[32] J. Andren, M. Hilding, D. Veitch, Understanding end-to-end internet traffic dynamics, GLOBECOM 1998, The Bridge to Global Integration 2 (1998) 1118–1122.
[33] M.S. Borella, G.B. Brewster, Measurement and analysis of long-range dependent behavior of internet packet delay, in: Proceedings of IEEE INFOCOM 1998, vol. 2, pp. 497–504.
[34] Q. Li, D.L. Mills, On the long-range dependence of packet round-trip delays in internet, ICC 98 2 (1998) 1185–1191.
[35] N.T.J. Bailey, The Mathematical Theory of Infectious Diseases and its Applications, Charles Griffin and Company, London, 1975.
[36] R.N. Bhattacharya, E.C. Waymire, Stochastic Processes with Applications, Wiley, New York, 1990.
[37] K. Calvert, M. Doar, E.W. Zegura, Modeling internet topology, IEEE Communications Magazine (June) (1997).
[38] GT-ITM topology generator. Available from: <http://www.isi.edu/nsnam/ns/ns-topogen.html>.
[39] I. Norros, Queuing behavior under fractional brownian traffic, in: K. Park, W. Willinger (Eds.), Self-Similar Network Traffic and Performance Evaluation, Wiley, New York, 2000.
[40] O.J. Boxma, J.W. Cohen, The single server queue: heavy tails and heavy traffic, in: K. Park, W. Willinger (Eds.), Self-Similar Network Traffic and Performance Evaluation, Wiley, New York, 2000.
[41] M. Çağlar, Ö. Özkasap, Multicast transport protocol analysis: self-similar sources, in: Proceedings of the 4th International IFIP-TC6 Networking Conference, LNCS 3042, Athens, Springer Verlag, Berlin, 2004, pp. 1294–1299.
[42] http://www.cubinlab.ee.mu.oz.au/~darryl/MS_code.html.
[43] A. Veres, M. Boda, The chaotic nature of TCP congestion control, IEEE INFOCOM (2000).
[44] K. Park, G.T. Kim, M.E. Crovella, On the relationship between file sizes, transport protocols, and self-similar

network traffic, in: Proceedings of the Fourth International Conference on Network Protocols, October 1996.
[45] Ö. Özkasap, Scalability, Throughput stability and efficient buffering in reliable multicast protocols, Technical Report, TR2000-1827, Department of Computer Science, Cornell University.
[46] M.S. Taqqu, W. Willinger, R. Sherman, Proof of a fundamental result in self-similar traffic modeling, Computer Communication Review 27 (1997) 5–23.
[47] Ö. Özkasap, M. Çağlar, Traffic Characterization of scalable multicasting in the case of a self-similar source (poster), ACM SIGCOMM, Karlsruhe, Germany, 25–29 August 2003.
[48] T. Konstantopoulos, S. Lin, Macroscopic models for long-range dependent network traffic, Queueing Systems 28 (1998) 215–243.

Öznur Özkasap received her M.S. and Ph.D. degrees in Computer Engineering, both from Ege University, in 1994 and 2000, respectively. During her Ph.D., she was awarded the TUBITAK-NATO A2 Ph.D. Research Scholarship Abroad and spent 1997–1999 at Cornell University, where she completed her Ph.D. dissertation. From 1992 to 2000, she has been a research and teaching assistant at Ege University, Department of Computer Engineering, and from 1997 to 1999 she has been as graduate research assistant at Cornell University, Department of Computer Science. Since 2000, she is an assistant professor in the Department of Computer Engineering of Koc University in Istanbul, Turkey. Her research interests include distributed computing systems, scalable reliable multicast protocols, peer-to-peer communication, protocol performance evaluation, and computer networks.

Mine Çağlar received her B.S. and M.S. degrees in Industrial Engineering from Middle East Technical University and Bilkent University, respectively. She received a Ph.D. degree in statistics and operations research from Princeton University in 1997. She worked as a post-doctoral research scientist at Bellcore in Morristown, in Network Design and Traffic Research Group during 1997–1998. She joined Koc University in 1999 where she works as an assistant professor of mathematics since then. Her current research interests are in the areas of stochastic flows and modeling of data traffic in telecommunications.